Human Molecular Genetics, 2015, Vol. 24, No. 13 3608–3622

doi: 10.1093/hmg/ddv106
Advance Access Publication Date: 19 March 2015
Original Article

ORIGINAL ARTICLE

Cardiac deficiency of single cytochrome oxidase assembly factor *scox* induces p53-dependent apoptosis in a *Drosophila* cardiomyopathy model

Leticia Martínez-Morentin[1], Lidia Martínez[1], Sarah Piloto[2], Hua Yang[3], Eric A. Schon[3], Rafael Garesse[1,4], Rolf Bodmer[2], Karen Ocorr[2,*], Margarita Cervera[1,4,*] and Juan J. Arredondo[1,4,*]

[1]Departamento de Bioquímica, Facultad de Medicina, Instituto de Investigaciones Biomédicas "Alberto Sols" UAM-CSIC and Centro de Investigación Biomédica en Red (CIBERER), c/ Arzobispo Morcillo s/n, Universidad Autónoma de Madrid, Madrid 28029, Spain, [2]Development, Aging and Regeneration Program, Sanford-Burnham Medical Research Institute, 10901 N Torrey Pine Rd, San Diego, CA 92037, USA, [3]Department of Neurology and Department of Genetics and Development, College of Physicians and Surgeons, Columbia University, 630 West 168th Street P&S 4-449, New York, NY, USA and [4]Instituto de Investigación Sanitaria Hospital 12 de Octubre (i+12), Madrid 28041, Spain

*To whom correspondence should be addressed. Tel: +34 914975402; Fax: +34 915854401; Email: juan.arredondo@uam.es (JJA). Tel: +34 914975402; Fax: ++34 915854401; Email: margarita.cervera@uam.es (MC). Tel: +1 8587955295; Fax: +1 8587955293; Email: kocorr@sanfordburnham.org (KO)

Abstract

The heart is a muscle with high energy demands. Hence, most patients with mitochondrial disease produced by defects in the oxidative phosphorylation (OXPHOS) system are susceptible to cardiac involvement. The presentation of mitochondrial cardiomyopathy includes hypertrophic, dilated and left ventricular noncompaction, but the molecular mechanisms involved in cardiac impairment are unknown. One of the most frequent OXPHOS defects in humans frequently associated with cardiomyopathy is cytochrome c oxidase (COX) deficiency caused by mutations in COX assembly factors such as Sco1 and Sco2. To investigate the molecular mechanisms that underlie the cardiomyopathy associated with Sco deficiency, we have heart specifically interfered scox expression, the single *Drosophila* Sco orthologue. Cardiac-specific knockdown of scox reduces fly lifespan, and it severely compromises heart function and structure, producing dilated cardiomyopathy. Cardiomyocytes with low levels of scox have a significant reduction in COX activity and they undergo a metabolic switch from OXPHOS to glycolysis, mimicking the clinical features found in patients harbouring Sco mutations. The major cardiac defects observed are produced by a significant increase in apoptosis, which is dp53-dependent. Genetic and molecular evidence strongly suggest that dp53 is directly involved in the development of the cardiomyopathy induced by scox deficiency. Remarkably, apoptosis is enhanced in the muscle and liver of Sco2 knock-out mice, clearly suggesting that cell death is a key feature of the COX deficiencies produced by mutations in Sco genes in humans.

Received: January 8, 2015. **Revised:** March 2, 2015. **Accepted:** March 17, 2015

Introduction

Mitochondrial respiratory chain disorders (MRCDs) due to dysfunctions in the oxidative phosphorylation (OXPHOS) system are among the most frequent inborn errors of metabolism, with an incidence of 1:5000 live births (1). MRCDs are multisystemic diseases and therefore, it is very difficult to distinguish systemic and tissue-specific phenotypes. Moreover, MRCDs are associated with a broad spectrum of clinical manifestations, with dilated or hypertrophic cardiomyopathies representing a common feature of these conditions. Neonatal cardiac abnormalities can be either isolated or accompanied by multi-organ involvement and are frequently associated with metabolic crises and lactic acidosis that may produce a fatal outcome (2).

Cytochrome c oxidase (COX) is the terminal component of the mitochondrial respiratory chain (MRC). COX is a multimeric complex comprised of 13 structural subunits whose assembly into a fully functional holoenzyme is a complicated process requiring accessory factors (3). Indeed, COX deficiency due to mutations in COX assembly factors is one of the most frequent causes of MRC defects in humans (4).

SCO1 and *SCO2* are paralogous genes that encode metallochaperones, both of which fulfil essential, non-overlapping cooperative roles in complex IV catalytic core assembly (5). In this way, these genes help maintain cellular copper homeostasis (6) and perhaps redox regulation (7). Pathogenic mutations in *SCO1* cause fatal infantile hepatoencephalomyopathy (8), although one such case with hypertrophic cardiomyopathy has been reported (9). Mutations in *SCO2* cause fatal infantile cardioencephalomyophathy, with all but one of the patients harbouring the E140 K mutation (10). Despite the similar functions of SCO1 and SCO2, their precise role in COX assembly remains unknown. Although SCO1 predominates in blood vessels, both are expressed ubiquitously, but it is intriguing that mutations in the two genes are associated with different tissue-specific COX deficiencies and distinct clinical phenotypes (11).

SCO2 synthesis is transcriptionally activated by p53, which has been shown to modulate the balance between OXPHOS and glycolysis (12). In addition, p53 appears to promote mitochondrial function and regulate metabolic homeostasis through different target genes, including *AIF*, *parkin*, *TFAM*, *POLγ* and *PGC1α* (13–17). Given the homeostatic relationships among these genes, it would seem likely that a feedback mechanism would exist between mitochondria and p53. In fact, it was recently shown in *Drosophila* competitive mosaics that p53 is not only induced as an adaptation to regulate mitochondrial respiration, but that it also plays an important role in metabolic homeostasis by enhancing glycolytic flux (18).

Here, we investigated the genetic and molecular mechanisms that underlie cardiomyopathies associated with SCO deficiency in *Drosophila*. Unlike vertebrates, *Drosophila* heart function can be significantly compromised without causing immediate death (19). Furthermore, since the genetic network controlling cardiac specification and differentiation are conserved from flies to mammals, as well as many other aspects of heart function, *Drosophila* has become a powerful genetic model to study cardiomyopathies (20–22).

In *Drosophila*, there is a single orthologue of mammalian *SCO1* and 2, *scox*, which has been identified and characterized (23). Ubiquitous *scox* knockdown (KD) or null mutant flies are lethal at larval stages, whereas weaker mutants are associated with motor dysfunction and female sterility. Indeed, such mutants display a strong disruption of Complex IV assembly and a concomitant reduction of COX enzyme activity (23,24). Here we demonstrate that cardiac-specific *scox* knockdown causes cardiomyopathy, severely compromising heart function and structure. We show that cardiomyocytes undergo a metabolic switch from OXPHOS to glycolysis, probably accompanied by enhanced lactic acid production, mimicking the clinical features of patients with SCO mutations. The major cardiac defects observed appear to be provoked by cell death, which is dp53-dependent. Significantly, we show that loss of p53 or inhibition of apoptosis blocks the Sco-induced cardiomyopathy. Our study shows strong evidence that dp53 is directly involved in the development of cardiomyopathy produced by SCOX partial loss of function.

Results

Cardiac-specific interference of *scox* causes mitochondrial impairment

To analyse the role played by SCO proteins in cardiomyopathies, we generated a *Drosophila* model based on heart-specific RNAi-mediated knockdown of *scox*. We first tested whether ubiquitous *scox* knockdown produced a phenotype similar to that described for *scox* homozygous mutants or its ubiquitous interference, as recently described (23,24). Ubiquitous knockdown of *scox* using the daughterless (Da::Gal4) driver and a UAS-scox RNAi (UAS-scoxi) resulted in animals developing only to the third-instar stage, never reaching pupal stage, and displaying a Spargel phenotype typical of mutations affecting mitochondrial proteins (Supplementary Material, Fig. S1A) (25,26). Moreover, *scox* silencing strongly impaired COX activity, whereas Complex I activity remained unaffected (Supplementary Material, Fig. S1B), demonstrating that ubiquitous interference of *scox* expression phenocopies its loss of function (23).

Cardiac-specific *scox* knockdown using *TinCΔ4::Gal4* as the driver also compromised *Drosophila* survival. *TinCΔ4-Gal4> scoxi* flies began to die after 2 weeks and had a mean lifespan 12 days shorter than controls (*TinCΔ4::Gal4/+*). Hence, all experiments were carried out on 1- or 2-week-old flies.

We evaluated the extent of *scox* KD by measuring mRNA expression in fly hearts by quantitative reverse transcriptase-polymerase chain reaction (qRT-PCR) and by histochemical staining of heart complex IV activity. We observed a 50% reduction in *scox* mRNA in hearts from 1-week-old *TinCΔ4-Gal4>scoxi* flies compared with the outcrossed driver and *UAS-scoxi* controls (Fig. 1A). We used complex IV activity histochemical staining to evaluate the extent of complex IV activity loss as consequence of *scox* KD (Fig. 1B, top row). There was a clear decrease in COX activity *in vivo* in *scox* KD semi-intact hearts from 1-week-old flies when compared with *TinCΔ4-Gal4* and *UAS-scoxi* controls. In order to confirm that the observed staining was in fact a consequence of Complex IV activity, hearts were stained in the presence of the COX inhibitor KCN. Inhibition of COX effectively prevented the staining (Fig. 1B, second row). To further corroborate that *scox* interference was causing an isolated COX deficiency, we also examined succinate dehydrogenase (SDH, CII) activity by histochemical staining. In this case, we observed no such differences in SDH activity between the *scox* KD and controls. Again, treatment of the samples with CII-specific inhibitor Malonate confirmed the staining specificity (Fig. 1B, lower rows). These results indicate that a decrease of just 50% in *scox* mRNA expression is sufficient to compromise COX activity in the *Drosophila* heart and that this defect is specific to Complex IV.

Mitochondrial dysfunction alters energy metabolism in many forms of heart disease (27) and therefore, we hypothesized that the COX deficiency displayed by cardiac-specific *scox* KD hearts should provoke a partial blockage of the citric acid cycle and a

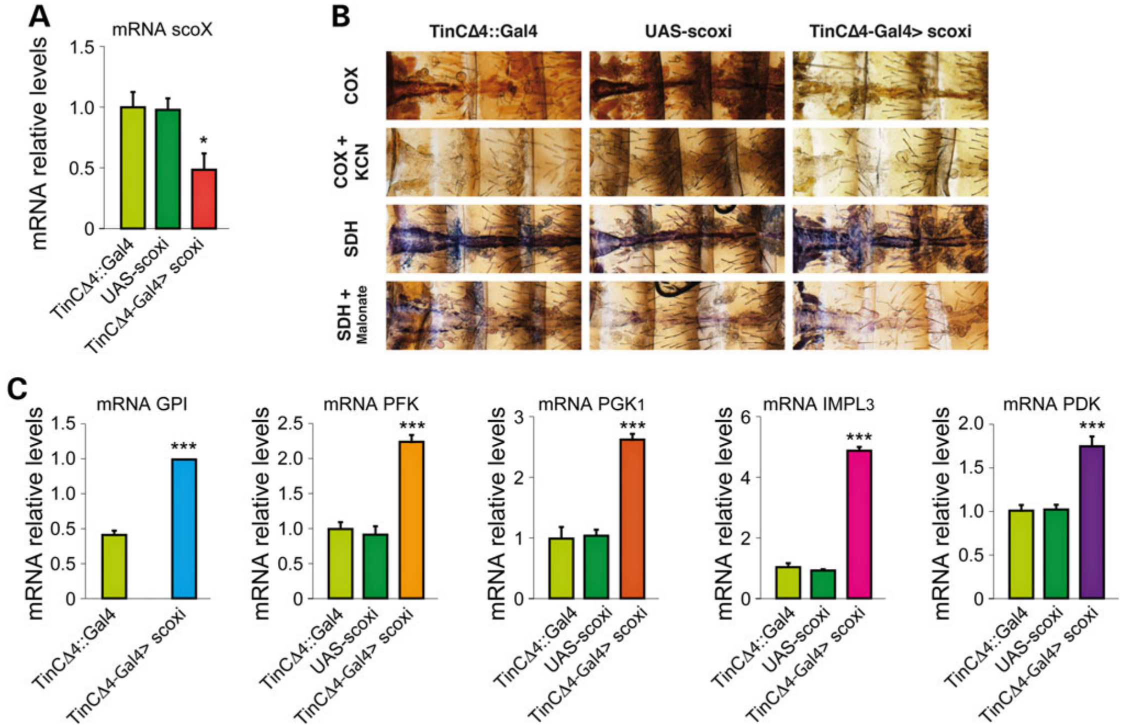

Figure 1. Cardiac-specific scox knockdown causes a mitochondrial impairment. (**A**) qPCR of *scox* RNA in 1-week-old adult hearts from cardiac scox KD hearts (TinCΔ4-Gal4 > scoxi) and controls from driver and UAS::RNAi lines (TinCΔ4::Gal4 and UAS-scoxi). Relative expression of *scox* in adult hearts was normalized to RpL10 expression. Control (TinCΔ4::Gal4) was set as one. Cardiac-specific scox KD showed 50% reduction compared with control. Values are displayed as mean ± SEM. Statistical significance was determined by unpaired, Student's two-tailed *t*-test: *$P < 0.05$. $n = 6–10$ per genotype. (**B**) Histochemistry from control hearts (TinCΔ4::Gal4 and UAS-scoxi) and cardiac-specific scox KD (TinCΔ4-Gal4>scoxi). Hearts were stained for CIV (COX), CII activities or combined activity stains with its inhibitor KCN (COX) and malonate (CII). Cardiac scox KD hearts present weaker COX staining than controls, whereas no differences in CII staining between scox KD and controls are observed. (**C**) Quantitative RT-PCR analysis of *GPI, PFK, PGK1, IMPL3* and *PDK* mRNA expression levels in 2-week-old adult hearts from cardiac scox KD hearts (TinCΔ4-Gal4 > scoxi) and controls (TinCΔ4::Gal4 and UAS-scoxi). Heart-specific scox KD leads to an increase in all measured transcript levels, suggesting a metabolic switch from glucose oxidation to glycolysis. mRNA levels are expressed relative to RPL10 as an internal control and relative to the TinCΔ4::Gal4 control. Values are displayed as mean ± SEM. Statistical significance was determined by unpaired, Student's two-tailed *t*-test: ***$P < 0.001$. $n = 6–10$ per genotype.

compensatory upregulation in glycolysis. We assessed the expression level of key enzymes involved in both glycolysis and citric acid cycle with qRT-PCR. We found that glycolytic enzymes, including glucose-6-phosphate isomerase (*gpi*), phosphofructokinase (*pfk*) and phosphoglycerate kinase (*pgk1*) were all upregulated in *TinCΔ4-Gal4>scoxi* KD hearts. Furthermore, expression of the *Drosophila* orthologue of human lactate dehydrogenase (LDH), *impl3* and the mitochondrial matrix enzyme pyruvate dehydrogenase kinase (*pdk*) were also enhanced (Fig. 1C). LDH converts pyruvate to lactate, the final product of non-respiratory glucose consumption, and its enhanced expression would be expected to result in lactic acidosis. PDK is a key regulator of glucose oxidation, inhibiting pyruvate dehydrogenase (PDH), thereby blocking entry of pyruvate into the citric acid cycle. Hence, our data strongly suggest that cardiac-specific interference of *scox* causes mitochondrial dysfunction, with the concomitant metabolic switch from glucose oxidation to glycolysis.

scox RNAi knockdown causes cardiomyopathy in *Drosophila melanogaster*

To assess how the mitochondrial dysfunction caused by silencing *scox* affects heart function, we used high-speed optical recording of semi-intact adult preparations of beating hearts and semi-automated analysis software to characterize cardiac physiology (28). Heart function in these flies is shown qualitatively in the M-mode traces from high-speed movies that illustrate heart wall movement over time (Fig. 2A). Hearts from 2-week-old controls showed regular rhythmic contractions, however, *TinCΔ4-Gal4>scoxi* hearts showed a distinctive slowing. The heart period ([HP]) was quantified from movies of beating hearts from 1- and 2-week-old *TinCΔ4-Gal4>scoxi* flies (Fig. 2B). *scox* KD resulted in a significantly increased HP (reduced heart rate, Fig. 2B and Supplementary Material, Fig. S2A). The increase in the heart period was due to a selective increase in the diastolic interval (DI: Fig. 2C), with 20% of the 2-week-old cardiac-specific *scox* KD flies displaying DIs longer than 1 s (Supplementary Material, Fig. S2B). In addition, in the region posterior to the conical chamber, the diastolic diameters of KD hearts were significantly smaller than controls. There was little effect on the average systolic diameter, consequently resulting in a significant reduction, from 43% in the controls to 33% in the *scox* KD flies, in heart tube contractility measured as fractional shortening (FS) (Fig. 2D–F). All cardiac parameters assessed in *scox* RNAi hearts were aggravated with age, and the phenotype observed was also dose-dependent, since animals harbouring just one copy of both driver and *UAS-scoxi* developed milder phenotypes (Fig. 2A, compare *TinCΔ4-Gal4>scoxi* to *TinCΔ4-Gal4/+>scoxi/+*). Thus, cardiac-specific *scox* knockdown results in severe cardiac dysfunction.

scox knockdown alters myofibril structure

The reduced contractility of the posterior heart tubes from *scox* KD flies led us to hypothesize that their heart structure might

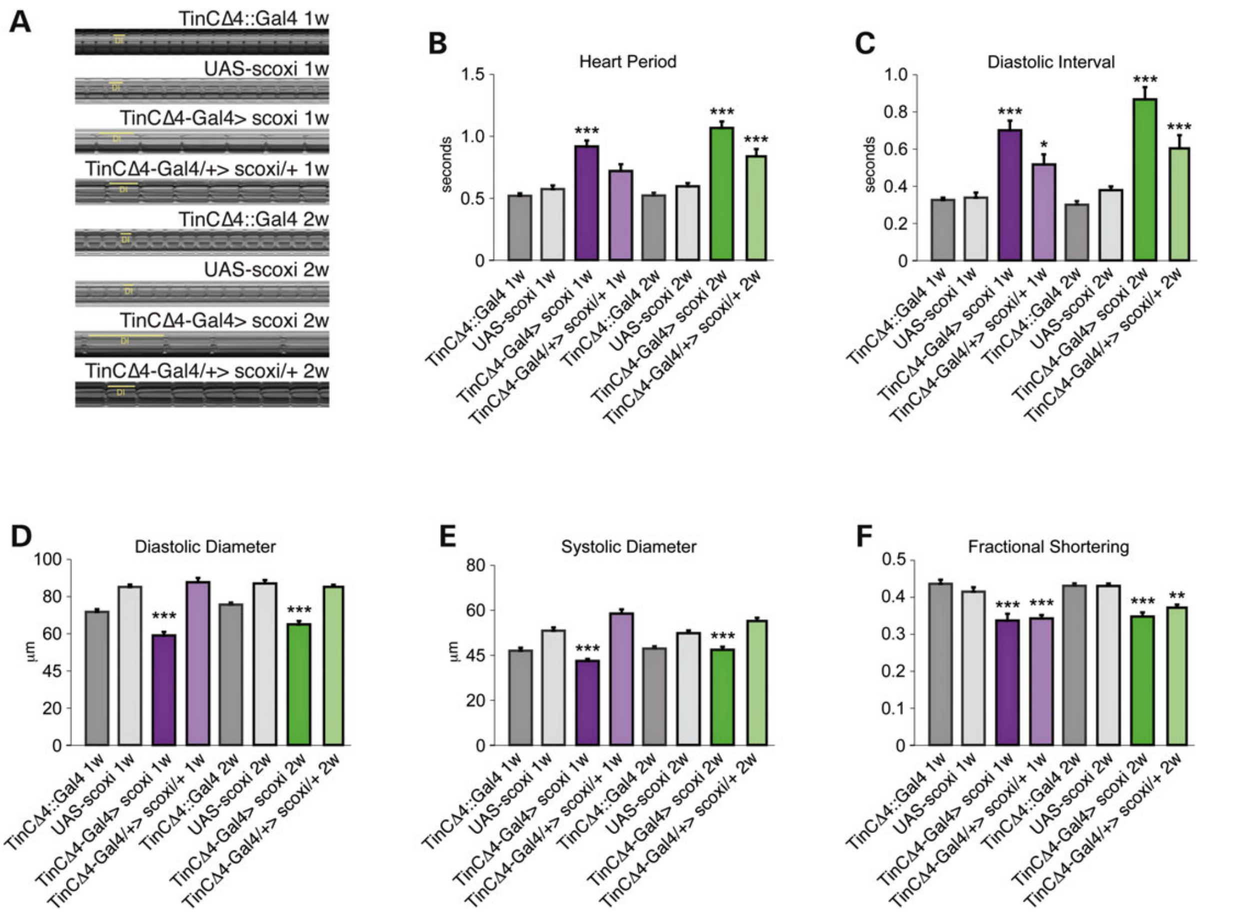

Figure 2. Cardiac-specific scox knockdown causes heart dysfunction. (**A**) Representative M-Mode traces (10 s) from high-speed movies of semi-intact *Drosophila* heart preparations. M-Mode traces represent the movements of the heart walls (y-axis) over time (x-axis). One- and two-week-old control flies (TinCΔ4::Gal4 and UAS-scoxi) present rhythmic heart beating. Cardiac-specific scox KD causes long DIs between contractions (DI, horizontal) in the homozygous and heterozygous lines compared with controls. scox KD hearts exhibit age-dependent deterioration in cardiac function. (**B**) Heart period, (**C**) DI, (**D**) diastolic diameter, (**E**) systolic diameter and (**F**) FS were measured for hearts from 1- and 2-week-old controls (TinCΔ4::Gal4 and UAS-scoxi) and cardiac-specific scox KD (TinCΔ4-Gal4>scoxi and TinCΔ4-Gal4/+>scoxi). Note the significant heart period and DI prolongation with scox KD in hearts from 1- and 2-week-old flies (TinCΔ4-Gal4>scoxi and TinCΔ4-Gal4/+>scoxi). Interestingly, hearts from double knockdown flies showed a significant decrease in systolic and diastolic diameters (TinCΔ4-Gal4>scoxi). FS is also significantly decreased due to a decreased systolic diameter and decrease in diastolic diameter. In all measures, the scox knockdown phenotype is more severe in 2-week-old flies. Significance was determined using a one-way ANOVA and Tukey's multiple comparisons post-hoc test. Differences are relative to the TinCΔ4::Gal4 control. Error bars indicate SEM (*$P < 0.05$, **$P < 0.01$ and ***$P < 0.001$). Sample size was 20–40 flies per genotype.

be altered. To explore the impact of silencing *scox* on heart structure, we used immunohistochemistry to examine *TinCΔ4-Gal4>scoxi* hearts from 1- and 2-week-old flies. Phalloidin staining revealed that although overall heart structure seemed to be fairly normal, *scox* RNAi animals exhibited myofibrillar disarray and an obvious narrowing of the heart tube from abdominal segment 4 to the end of the heart tube (arrows in Fig. 3A). This phenotype became more noticeable with age (Fig. 3A, compare 1 and 2 weeks). In addition, the size of the conical chamber diameter increased significantly in 1-week-old *TinCΔ4-Gal4>scoxi* flies compared with controls (Fig. 3B), suggesting that heart-specific *scox* interference causes dilated cardiomyopathy in *Drosophila*.

We then analysed the myofibrillar organization in phalloidin-stained cardiomyocytes from abdominal segments 3 (A3) and 4 (A4) in 1- and 2-week-old flies. This was the region where we observed a significant reduction in contractility in our functional assays. Cardiomyocytes from controls (*TinCΔ4::Gal4* and *UAS-scoxi*) displayed tightly packed and well-aligned circumferential myofibrils (Fig. 3C and D, 1–2), whereas myofibrils from cardiomyocytes in *TinCΔ4-Gal4>scoxi* hearts were loosely packed and poorly organized, being fully disorganized in those hearts displaying the stronger structural phenotypes (Fig. 3C and D, 3–4). Consistent with the overall morphology observed previously (Fig. 3A), fibre disorganization was strongest in the posterior half (compare A3 and A4 segments, Fig. 3C and D). Moreover, hearts from 2-week-old flies displayed more severe myofibrillar disarray than those from 1-week-old flies, with the heart tube often appearing almost collapsed (Fig. 3C 3–4′ and D 3–4′).

As one case of fetal wastage harbouring SCO2 mutations has been reported in humans (29), we wondered whether the structural defects observed in *TinCΔ4-Gal4>scoxi* heart tube were the consequence of a developmental or pupal heart-remodelling defect or whether the degenerative phenotype described was a consequence of the detrimental consequences of mitochondrial dysfunction accumulating over time. To test the former hypothesis, we used immunohistochemistry to examine cardiac-specific *scox* KD and control hearts from red-eyed pupae. Phalloidin staining revealed that the heart tubes from *TinCΔ4-Gal4>scoxi* pupae exhibited normal heart structure when compared with control hearts (Supplementary Material, Fig. S3), ruling out the possibility that a developmental or pupal heart-remodelling defect provoked the myofibril disorganization observed in the adult heart.

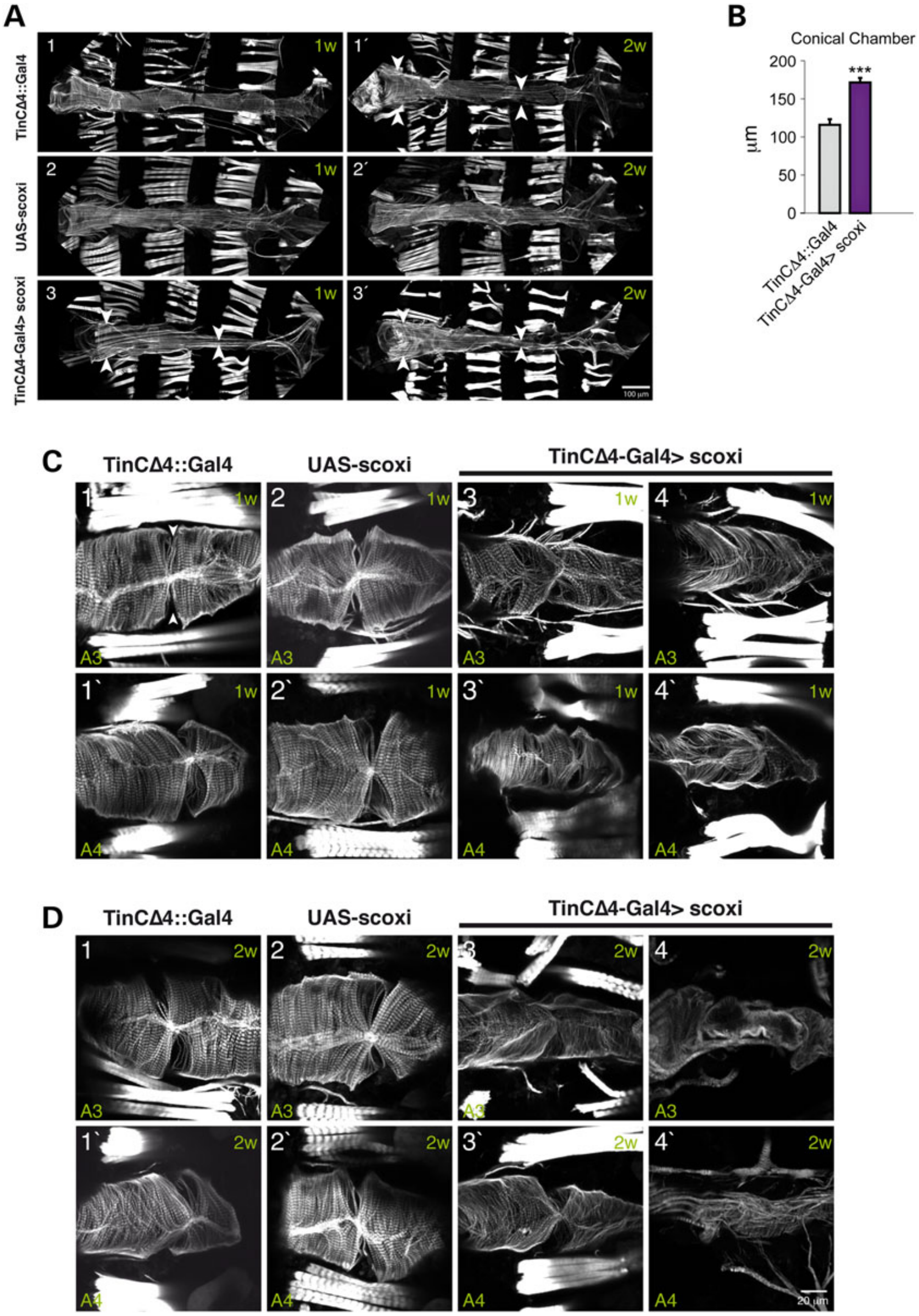

Figure 3. Cardiac-specific scox KD affects heart tube structure. **(A)** (1–3′) Confocal images of 1- and 2-week-old adult hearts stained with Alexa Fluor 594-phalloidin to identify actin filaments at 10× magnification. (1–2) Control hearts (TinCΔ4::Gal4 and UAS-scoxi) reveal normal conical chamber, cardiac tube diameter (arrows in 1–1′) and regular myofibrillar organization within the cardiomyocytes. (3–3) Cardiac-specific scox knockdown hearts show wider conical chamber, narrower tube diameter (arrows in 3–3) and myofibrillar disorganization. Arrowheads indicate the conical chamber and A4 segment. **(B)** Measurement of conical chamber diameter in 1-week-old adult hearts from control (TinCΔ4::Gal4) and cardiac-specific scox KD. Note that the conical chamber from cardiac-specific scox KD flies is significantly wider. Values are mean ± S.D. (error bars). Statistical significance was determined using multivariance Student's *t*-test (***$P < 0.0001$) ($n = 10$). Representative confocal images of third and fourth abdominal segments (A3 and A4) of the dorsal vessel from 1-week-old **(C)** and 2-week-old **(D)** flies at 25× optical magnification (2× ZOOM). Adult hearts are stained with Alexa Fluor 594-phalloidin to identify actin filaments. **(C,** 1–2′) **(D,** 1–2′) Cardiomyocytes from wild-type controls (TinCΔ4::Gal4 and UAS-scoxi) contain densely packed and circumferentially organized myofibrils **(A,** 3–4′) **(B,** 3–4′) Cardiac-specific scox KD flies causes overall disorganization with gaps between myofibrils that becomes more severe with age. The myofibrillar disorganization is more noticeable in the A4 abdominal segment with regions that lack myofibrils.

Together with data obtained from live beating hearts, these results suggest that *scox* downregulation compromises heart function and structure in a time-dependent manner that it is not due to developmental defects.

COX deficiency enhanced the production of reactive oxygen species

Mitochondrial respiration, mainly at electron transport chain (ETC) complexes I and III, is the main source of reactive oxygen

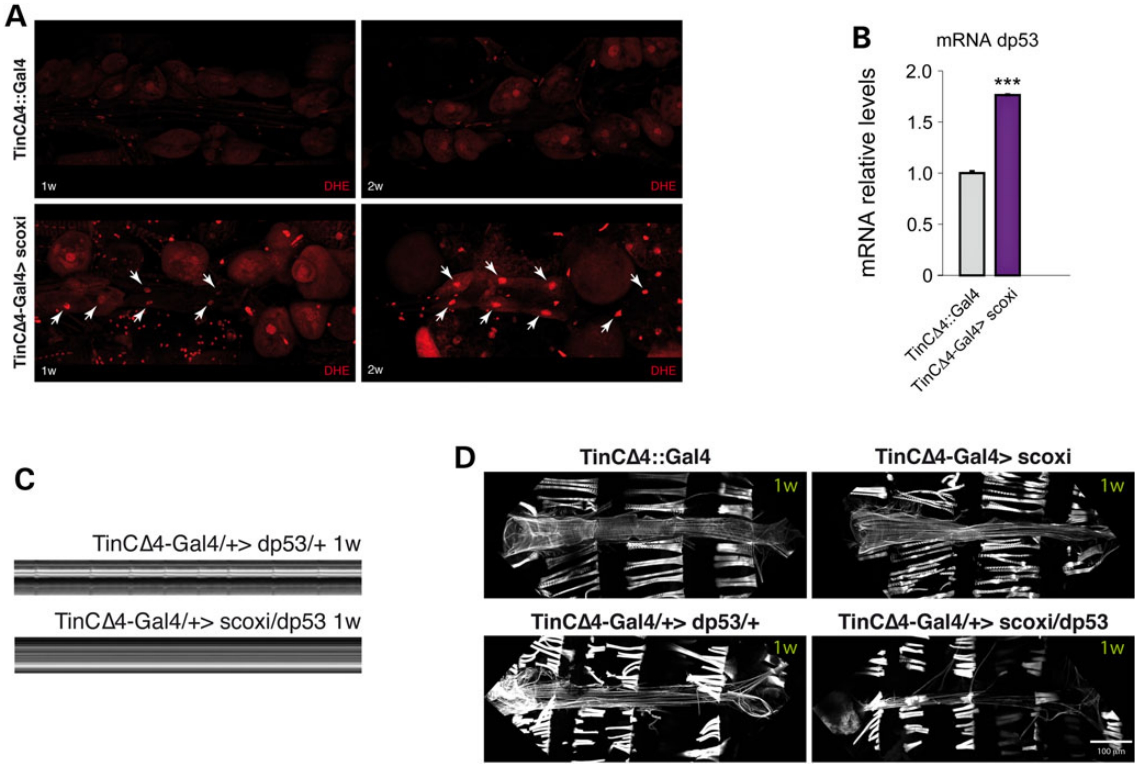

Figure 4. Cardiac-specific scox knockdown induces oxidative stress and p53-dependent heart degeneration. **(A)** Immunofluorescence micrographs showing DHE staining in hearts from control (TinCΔ4::Gal4) and cardiac-specific scox knockdown of 1- and 2-week-old adult hearts. DHE staining is enhanced in cardiac-specific scox KD compared with control. Thin arrows indicate DHE staining in the nuclei of scox KD cardiomyocytes. **(B)** qPCR of *p53* RNA in 1-week-old adult hearts from cardiac scox KD hearts (TinCΔ4-Gal4>scoxi) and control (TinCΔ4::Gal4). Relative expression of *p53* in adult hearts was normalized to RpL10 expression. Control (TinCΔ4::Gal4) was set as one. Cardiac-specific scox KD showed an increased in *p53* levels compared with control. Values are displayed as mean ± SEM. Statistical significance was determined by unpaired, Student's two-tailed *t*-test: ***$P < 0.001$. $n = 4$ per genotype. **(C)** Representative M-Mode traces (10 s) from high-speed movies of semi-intact flies preparations. *dp53* OE in cardiac-specific scox KD 1-week-old adult exhibited lack of heart beat. $n = 18$ experiments per genotype. **(D)** Confocal images of 1-week-old adult hearts stained with Alexa Fluor 594-phalloidin to identify actin filaments at 10× magnification. Control heart (TinCΔ4::Gal4), hearts from scox double knockdown flies ((TinCΔ4-Gal4>scoxi) and *dp53* OE flies (TinCΔ4-Gal4/+>dp53/+ and TinCΔ4-Gal4/+>scoxi/p53) are showed. *dp53* causes a dramatic myofibrillar disorganization with lack of cardiac spiral myofibers (second panel on the right).

species (ROS) in most eukaryotic cells (30), and an increase in ROS levels represents a source of cellular stress often associated with mitochondrial dysfunction (31). Interestingly, ROS formation and oxidative DNA damage have been shown to be enhanced in human $SCO2^{-/-}$ cells (32). As heart-specific *scox* knockdown causes mitochondrial dysfunction, we asked whether reduced COX activity augments ROS production. ROS levels were measured in hearts from 1- and 2-week-old control and cardiac-specific *scox* KD flies using dihydroethidium (DHE), a dye that is accumulated in the nucleus after reaction with superoxide anions, as an indicator. The stronger nuclear staining (arrowheads in Fig. 4A) in hearts from *TinCΔ4-Gal4>scoxi* indicated an increase in ROS production in *scox* KD hearts. In addition, DHE staining was stronger in cardiomyocytes from 2-week-old flies, indicating that ROS production, and therefore cellular stress, increased with age in *scox* KD hearts.

scox cardiomyopathy is p53-dependent

The p53 tumour suppressor plays a central role in cancer development, apoptosis, necrosis, senescence and differentiation, fulfils an important role in cellular stress response and regulates metabolic pathways such as glycolysis and OXPHOS (33). Furthermore, a number of studies have implicated p53 in different types of cardiomyopathies (34,35). Interestingly, *p53* directly regulates aerobic respiration in the stress response by modulating *Sco2* (12). In this context, since OXPHOS is partially compromised and the glycolytic pathway is upregulated in *scox* KD hearts, we hypothesized that *dp53*, the *Drosophila* homologue of *p53* (36), might also participate in the *Drosophila* stress response and the development of cardiomyopathy in *scox* KD hearts. We examined *p53* expression using qRT-PCR on hearts from 1-week-old flies, observing a significant increase in *dp53* transcripts in cardiac-specific *scox* KD hearts (Fig. 4B) further supporting that p53 may play a central role in the development of cardiomyopathy in *scox* KD hearts.

To complete our analysis of the role of dp53 in *scox* KD-associated cardiomyopathy, we co-overexpressed *dp53* in *TinCΔ4-Gal4>scoxi* KD hearts using a *UAS-dp53* line. We first examined the cardiac physiology of 1-week-old *TinCΔ4-Gal4/+>scoxi* KD/*dp53* overexpression (OE) flies to assess the effect of *dp53* OE and to determine whether there was any genetic interaction between *dp53* and *scox*. Overexpression of *dp53* alone caused a significant slowing of the heart period, reminiscent of *scox* KD. Surprisingly, we observed no heartbeat in *scox* KD hearts that were also overexpressing *p53* even at relatively young ages (1 week, Fig. 4C). Structural analyses by phalloidin staining of *TinCΔ4-Gal4/+>dp53/+* hearts revealed that *dp53* OE itself caused cardiac defects comparable to that of *scox* KD harbouring two copies of both driver and *UAS-scox* (Fig. 4D). Significantly, hearts from *TinCΔ4-Gal4/+>scoxi* KD/*dp53* OE flies exhibited very strong heart degeneration, with the complete loss of cardiac myofibrils and the presence of only a few longitudinal myofibrils from the dorsal longitudinal muscle in the animals displaying the strongest phenotypes. Note that in contrast, the animals that carried just one copy of each driver and *UAS-scoxi*, but no *UAS-dp53* (*TinCΔ4-Gal4/+>scoxi/+*), displayed a relatively mild phenotype (Fig. 6E).

It is possible that the cardiac degeneration observed in response to *dp53* OE in *scox* KD flies might be due to a general stress response triggered by mitochondrial impairment rather than a specific genetic interaction between *scox* and *dp53*. To clarify this possibility, we examined the cardiac response to KD of another complex IV assembly factor, Surf1. Knockdown of *Drosophila Surf1* gene expression has previously been shown to cause COX deficiency, with nervous system involvement and developmental arrest (37). We tested whether *dp53* OE in cardiac-specific *Surf1* KD animals caused a similar cardiac degeneration to that observed in *TinCΔ4-Gal4/+>scoxi/dp53* flies. We evaluated the extent of *Surf1* KD by measuring mRNA expression levels in fly hearts by qRT-PCR. Hearts from 1-week-old cardiac-specific Surf1 flies showed a 50% reduction in *Surf1* mRNA similar to that observed in *scox* KD hearts (Supplementary Material, Fig. S4A). Next, we asked whether reduced COX activity, a consequence of *Surf1* knockdown, augments ROS production as occurred in *scox* KD. ROS levels were measured in hearts from 2-week-old control and cardiac-specific *Surf1* KD flies using DHE. The stronger nuclear staining (arrowheads in Supplementary Material, Fig. S4B) in hearts from *TinCΔ4-Gal4>Surf1i* indicated an increase in ROS production in these hearts. Surprisingly, morphological analyses showed that 1-week-old Surf1 KD animals displayed only a very mild, if any, cardiac phenotype. Most remarkably, *TinCΔ4-Gal4/+>Surf1i* KD/*dp53* OE hearts looked entirely normal demonstrating that, unlike for *scox* KD, *Surf1* heart-specific KD not only has minimal effects on heart function, but appears to rescue the *dp53* OE heart phenotype (Supplementary Material, Fig. S4C). Furthermore, in contrast to our observations for *scox* KD hearts, we found no increase in *dp53* transcripts in *TinCΔ4-Gal4>Surf1i* hearts (Supplementary Material, Fig. S4D).

These results demonstrate that *dp53* and *scox* interact genetically, suggesting that dp53 might play an important role in the development of *scox* KD-induced cardiomyopathy.

Cardiac-specific knockdown of scox induces apoptosis

Given the pro-apoptotic activity of dp53 (36,38), it would appear that *scox* knockdown might induce dp53-dependent apoptosis in cardiomyocytes. As dp53 controls cell death through the Reaper-Hid-Grim network (39), we assessed their relative expression and we observed a significant increase in *Reaper*, *Hid* and *Grim* mRNA expression in heart tubes from 1- and 2-week-old *TinCΔ4-Gal4>scoxi* flies (Fig. 5A), reflecting the activation of the apoptotic pathway in *scox* KD flies. Whether the cardiac defects caused by *scox* interference might be due to apoptosis activation was further assessed by terminal deoxynucleotidyl transferase dUTP nick end labelling (TUNEL) staining in hearts from 1- and 2-week-old *scox* KD flies. Although no TUNEL labelling was evident in control hearts from 1- or 2-week-old animals (Fig. 5B, 1 and 3), clear labelling was observed in 1-week-old cardiac-specific *scox* KD hearts (Fig. 5B, 2), which was markedly stronger after 2 weeks (Fig. 5B, 4). To confirm whether apoptosis was responsible for the structural disarray observed in *scox* KD hearts, we overexpressed the pro-apoptotic gene *Reaper* in a *TinCΔ4-Gal4>scoxi* background. Hearts from these 1-week-old *TinCΔ4-Gal4>scoxi,rpr* flies presented strong myofibril disorganization (Supplementary Material, Fig. S5A and B) reminiscent of that observed in 2-week-old cardiac-specific *scox* KD flies. Together, these data clearly demonstrate that cardiac-specific *scox* KD activates apoptosis, inducing cell death.

Disruption of dp53 activity rescues *scox* cardiomyopathy

The fact that *scox* downregulation triggers dp53-mediated apoptosis, together with the strong degeneration observed in those flies, which is exacerbated by dp53 OE, led us to hypothesize that blocking the dp53 pathway might impede apoptosis and rescue cardiac function in *TinCΔ4-Gal4>scoxi* flies. We used a dominant-negative form of *dp53* (*UAS-dp53^{DN}*, *dp53^{DN}*) to abrogate p53 activity in a *scox* KD background. M-Mode records from *TinCΔ4-Gal4/+>scoxi/dp53^{DN}* and *TinCΔ4-Gal4/+>dp53^{DN}/+* 2-week-old fly hearts show regular rhythmic contractions and an average heartbeat length (Fig. 6A, compare with Fig. 2A). Furthermore, the quantification of the different physiological parameters showed that the DI and heart period of *TinCΔ4-Gal4/+>scoxi/dp53^{DN}* hearts were similar to that of controls and significantly shorter than that of *scox* KD hearts (Fig. 6B). FS, an indicator of heart contractibility, was also rescued by *dp53^{DN}* expression in *scox* KD hearts (Fig. 6B), demonstrating that heart activity was fully rescued by disruption of dp53 activity.

When we examined cardiac structure, there were no obvious morphological defects in the hearts of 2-week-old flies overexpressing *dp53^{DN}* alone, or in the hearts from cardiac-specific *scox* KD animals that also overexpressed *dp53^{DN}*. Specifically, the myofibrillar arrangement within the cardiomyocytes of *TinCΔ4-Gal4/+>scoxi/dp53^{DN}* or *TinCΔ4-Gal4>scoxi/dp53^{DN}* flies, respectively, carrying one or two driver copies, were circumferentially aligned (Fig. 6C). Under higher magnification, the structure of the A3 and A4 segments demonstrated that cardiac-specific overexpression of *dp53^{DN}* fully restored the severe morphological defects found in *scox* KD (Fig. 6D).

It could be argued that the observed rescue might be explained by the presence of a second UAS in *TinCΔ4-Gal4/+>scoxi/dp53^{DN}* flies which could result in a weaker interference of *scox* expression. In order to rule out this possibility, we expressed the unrelated protein GFP (*UAS-GFP*) in *TinCΔ4-Gal4>scoxi* flies. Animals harbouring one copy of *TinCΔ4::Gal4* to drive the expression of both *gfp* and *scoxi* (*TinCΔ4-Gal4/+>scoxi/GFP*) still displayed structural defects comparable to those displayed by *TinCΔ4-Gal4/+>scoxi/+* (Fig. 6C and D), indicating that the cardiac dysfunction rescue was not due to a weaker interference but rather to a blockage of the p53 pathway (Fig. 6B).

To further demonstrate the involvement of dp53 in the development of cardiomyopathy, we disrupted *scox* expression in a *dp53* null background. The heart-specific KD of *scox* in a *dp53$^{-/-}$* flies did not provoke myofibrillar disarray or any other defect (Supplementary Material, Fig. S6A), further emphasizing the role of p53 in the development of scox-mediated cardiomyopathy.

We also asked whether inhibiting apoptosis would rescue the structural degeneration observed in cardiac-specific *scox* KD cardiomyocytes. This was assessed by expressing the baculovirus caspase inhibitor *p35* (40) or the *Drosophila* inhibitor of apoptosis *DIAP1* (41) in a cardiac-specific *scox* KD background. Two-week-old *scoxi* KD flies expressing *p35* or *DIAP1* in a heart-specific manner showed no structural defects (Supplementary Material, Fig. S7A), although under higher magnification, mild disarray was observed when *DIAP1* was overexpressed (Supplementary Material, Fig. S7B). Thus, inhibiting apoptosis appears to rescue the myofibrillar degeneration observed in *scox* KD flies.

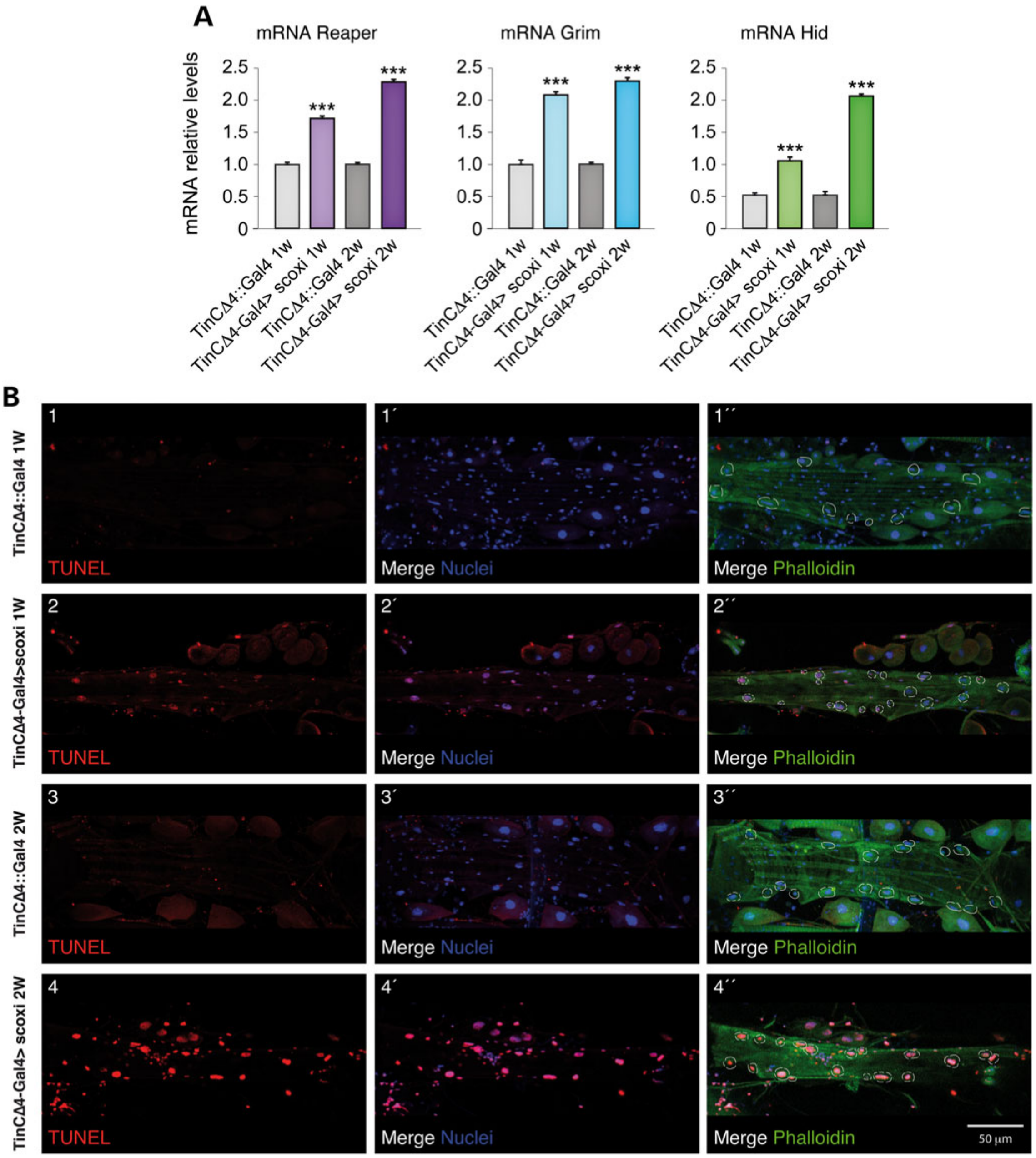

Figure 5. Cardiac-specific scox knockdown induces apoptosis. (**A**) qPCR of *Reaper*, *Grim* and *Hid* RNA in 1- and 2-week-old adult hearts from cardiac scox KD hearts (TinCΔ4-Gal4>scoxi) and control (TinCΔ4::Gal4). Transcript levels were normalized to RPL0 expression. Control (TinCΔ4::Gal4) was set as one. Cardiac-specific scox KD showed an increased in *Reaper*, *Grim* and *Hid* levels compared with control. Values are displayed as mean ± SEM. Statistical significance was determined by unpaired, Student's two-tailed *t*-test: ***$P < 0.001$. $n = 5$–8 experiments per genotype. (**B**) Assessment of cardiomyocytes apoptosis *in vivo* by TUNEL staining in 1- and 2-week-old adult hearts from cardiac scox KD hearts (TinCΔ4-Gal4>scoxi) and control (TinCΔ4::Gal4) at 25× optical magnification. TUNEL-positive nuclei (red), DAPI (blue) and Alexa Fluor 488 phalloidin (green, merge) (2,4). Cardiac-specific scox KD causes apoptosis in at least 50% of the nuclei in a 50% of the hearts from 1-week-old flies and in an 80% in hearts from 2-week-old flies. Cardiomyocyte nuclei are encircled in white (merge). Sample size was 15–20 flies per genotype.

Sco2^{KIKO} mice undergo apoptosis

In light of the above data, we wondered whether our results in the *Drosophila* heart could be extended to mammals. Although there are no *Sco1* KO mice currently available, a *Sco2*$^{KI/KO}$ mouse model has been recently developed that harbours a *Sco2* knock-out allele and the *Sco2* knock-in E129 K allele which corresponds to the E140 K mutation found in almost all human patients (31). As observed in patients with SCO2 deficiency, these *Sco2*$^{KI/KO}$ mice display motor impairments, as well as biochemical and functional defects. It should be noted that, in contrast to humans, the reduction in COX activity in *Sco2*$^{KI/KO}$ mice was less severe in muscle than in other tissues, such as liver, and it was accompanied by an unexpected defect in complex III activity (31). *Sco2*$^{KI/KO}$ mice do not develop overt symptoms of the cardioencephalomyopathy seen in the human disease and no significant differences in cardiac function between WT and Sco2-mutated mice, as measured by transthoracic M-mode and two-dimensional echocardiography (31). Therefore, we decided to analyse whether there was apoptosis in liver and skeletal muscle, the two most

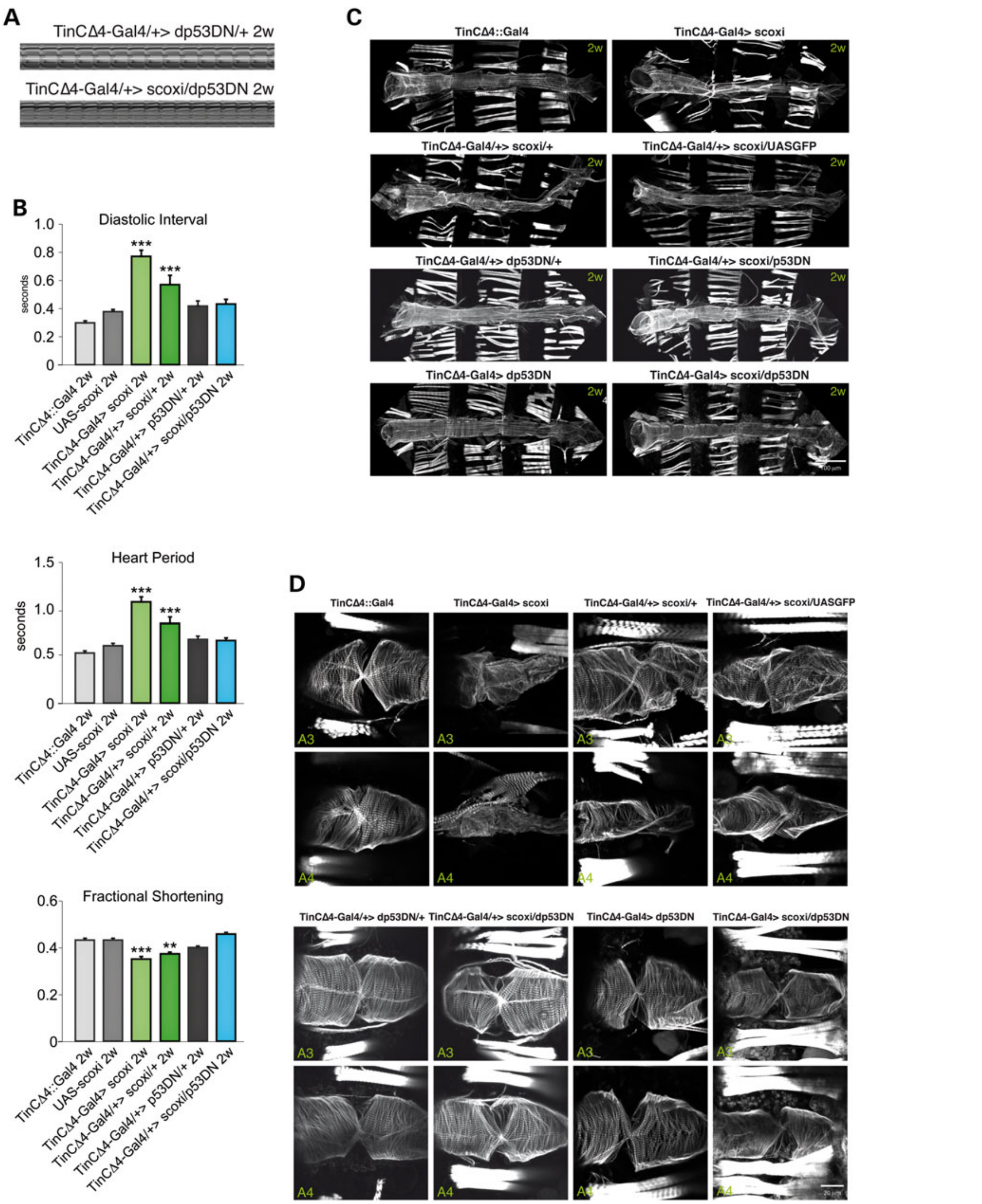

Figure 6. Lack of dp53 activity rescues scox cardiomyopathy. (**A**) Representative M-Mode traces (10 s) from high-speed movies of semi-intact flies. Cardiac-specific dp53^{DN} OE in 2-week-old scox KD hearts (TinCΔ4-Gal4/+>scoxi/ dp53^{DN}) causes a significant enhancement in cardiac function compared with that seen in response to cardiac-specific scox KD alone (Fig. 2). Cardiac-specific dp53^{DN} OE in 2-week-old hearts (TinCΔ4-Gal4/+>dp53^{DN}/+) does not affect heart function. (**B**) DI, heart period and FS were measured for hearts from 2-week- old controls (TinCΔ4::Gal4 and UAS-scoxi), cardiac-specific scox KD (TinCΔ4-Gal4>scoxi and TinCΔ4-Gal4/+>scoxi/+) and *dp53*^{DN} OE (TinCΔ4Gal4/+>dp53^{DN}/+ and TinCΔ4Gal4/+>scoxi, dp53^{DN}). In all measures, cardiac-specific *dp53*^{DN} OE rescues the scox knockdown phenotype in 2-week-old flies. Significance was determined using a one-way ANOVA and Tukey's multiple comparisons post-hoc test. Differences are relative to the TinCΔ4::Gal4 control. Error bars indicate SEM ($^{**}P < 0.01$ and $^{***}P < 0.001$). Sample size was 20–40 flies per genotype. (**C**) Confocal images of 2-week-old adult hearts stained with Alexa Fluor 594-phalloidin to identify actin filaments at 10× magnification. Hearts from control (TinCΔ4::Gal4), cardiac-specific scox KD (TinCΔ4-Gal4>scoxi and TinCΔ4-Gal4/+>scoxi/+) and cardiac-specific *dp53*^{DN} OE (TinCΔ4Gal4>dp53^{DN}, TinCΔ4Gal4/+>dp53^{DN}/+, TinCΔ4Gal4>scoxi,dp53^{DN} and TinCΔ4Gal4/+>scoxi,dp53^{DN}) are shown. Cardiac-specific *dp53*^{DN} OE (third and fourth panels on the right) rescues the scox KD structural phenotype (first and second panels on the right and second panel on the left). Controls expressing *dp53*^{DN} (TinCΔ4Gal4/+>dp53^{DN}/+ and TinCΔ4Gal4>dp53^{DN}) are shown in third and fourth panels on the left. (**D**) Representative confocal images of third and fourth abdominal segments (A3 and A4) of the dorsal vessel from 2-week-old flies at 25× optical magnification (2× ZOOM). Adult hearts are stained with Alexa Fluor 594-phalloidin to identify actin filaments. Cardiac-specific *dp53*^{DN} OE rescues myofibrillar disorganization caused by scox KD. Cardiomyocytes from cardiac-specific *dp53*^{DN} OE (TinCΔ4Gal4>scoxi,dp53^{DN} and TinCΔ4Gal4/+>scoxi,dp53^{DN}) exhibit regular circumferential myofibrillar arrangement (second-line panels, second and fourth lines).

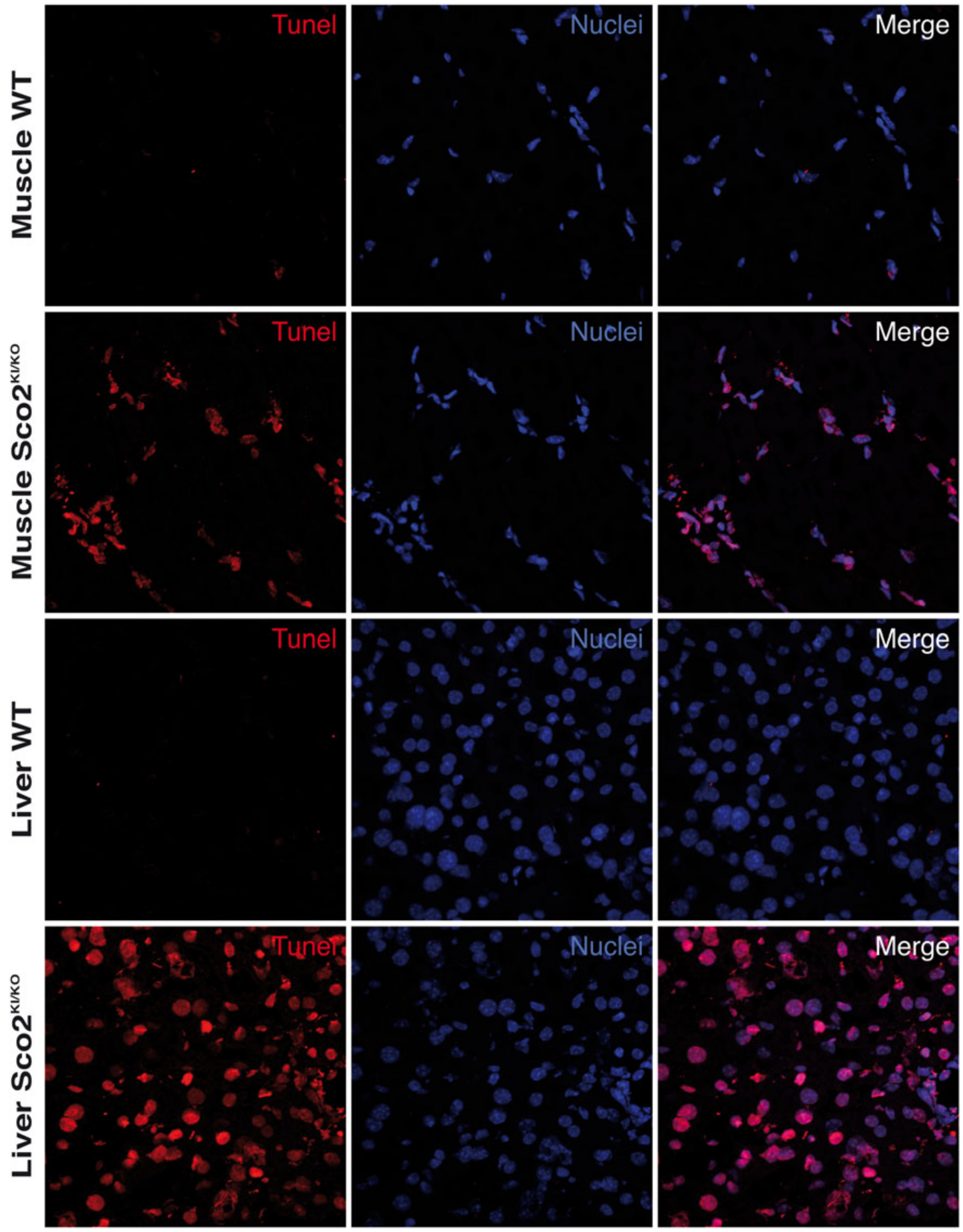

Figure 7. *Sco2*^{KIKO} mice undergo apoptosis in liver and skeletal muscle. Confocal images of control and *Sco2*^{KIKO} 6-month-old mice at 25× optical magnification. Skeletal muscle and liver were stained for TUNEL (red) and DAPI (blue). *Sco2*^{KIKO} mice show high levels of TUNEL-positive fluorescent red nuclei staining (second and fourth line panels). $n = 3$ per genotype.

affected tissues. TUNEL staining of liver and skeletal muscle from *Sco2*$^{KI/KO}$ mice revealed that there was extensive apoptosis in both tissues in *Sco2*$^{KI/KO}$ mice but not in WT animals (Fig. 7). Furthermore, the liver of *Sco2*$^{KI/KO}$ mice seemed to have more apoptotic cells than the muscle tissue, in agreement with previous observations that the liver has the lowest complex IV activity compared with other tissues in these mice (31). Hence, we conclude that, partial loss of Sco2 function in mice induces apoptosis, as we have observed in *Drosophila*.

Discussion

Cardiomyopathies are a collection of myocardial disorders in which the heart muscle is structurally and functionally abnormal. In the past decade, it has becomes clear that an important proportion of cases of hypertrophic and dilated cardiomyopathies are caused by mutations in genes encoding sarcomeric or desmosomal proteins. In addition, cardiomyopathies (both hypertrophic and dilated) are frequently associated to syndromic and non-syndromic mitochondrial diseases. The importance of oxidative metabolism for cardiac function is supported by the fact that 25–35% of the myocardial volume is taken by mitochondria. The current view of mitochondrial involvement in cardiomyopathy assumes that ETC malfunction results in an increased ROS production, triggering a “ROS-induced ROS release” vicious circle which in turn perpetuates ETC dysfunction via damage in mtDNA and proteins involved in electron transport. Under this view, accumulated mitochondrial damage would eventually trigger apoptosis through mitochondrial permeability transition pore (mPTP) opening other mechanisms (42). Under normal circumstances, damaged mitochondria would be eliminated through mitophagy. Excessive oxidative damage is supposed to overcome the mitophagic pathway resulting in apoptosis (43). Nevertheless, although several potential mechanisms have been suggested, including apoptosis deregulation, oxidative stress, disturbed calcium homeostasis or impaired iron metabolism, the molecular basis of the pathogenesis of mitochondrial cardiomyopathy is virtually unknown.

Pathogenic mutations in human *SCO1* and *SCO2* have been reported to cause hypertrophic cardiomyopathy, among other clinical symptoms (8,44). However, the molecular mechanisms underlying this cardiac dysfunction have yet to be elucidated. We present here the first cardiac-specific animal model to study human SCO1/2-mediated cardiomyopathy. Cardiac-specific *scox* KD provokes a severe dilated cardiomyopathy, as reflected by a significant increase in the conical chamber size, due to mitochondrial dysfunction. It presents a concomitant metabolic switch from glucose oxidation to glycolysis and an increase in ROS levels, leading to p53-dependent cell death. Interestingly, previous studies on patients and rat models have shown that mitochondrial dysfunction is associated with abnormalities in cardiac function and changes in energy metabolism, resulting in glycolysis optimization and lactic acidosis [(45) reviewed in Refs. (2,46)]. Furthermore, in the *Sco2*$^{KI/KO}$ mouse model, where no evidence of cardiomyopathy was described (31), partial loss of Sco2 function induces apoptosis in liver and skeletal muscle. In flies *scox* KD causes a significant reduction in FS and in the DI, as well as cardiac myofibril disorganization. This degenerative process was most likely due to mitochondrial dysfunction rather than to a developmental defect and moreover, the dilated cardiomyopathy developed by flies resembled that caused by mitochondrial fusion defects in flies (47,48).

The ETC is the major site of ROS production in cells (30), and aging and many neurodegenerative diseases have been linked to mitochondrial dysfunction that results in excessive oxidative stress (49). Interestingly, there is an increase in ROS formation associated with oxidative DNA damage in human *Sco2*$^{-/-}$ cells (32). Accordingly, we found that cardiac-specific knockdown of *scox* increases oxidative stress, although we cannot distinguish whether this increase in free radical accumulation arises from the mitochondria or whether it comes from non-mitochondrial sources due to a loss of cellular homeostasis, as reported in yeast (50) and in a neuro-specific COX-deficient Alzheimer disease mouse model (51).

Sco2 expression is known to be modulated by p53, a transcription factor that participates in many different processes, including cancer development, apoptosis and necrosis (reviewed in Ref. 52). p53 regulates homeostatic cell metabolism by modulating *Sco2* expression (12,33) and contributes to cardiovascular disorders (34,35). In addition, p53 activation in response to stress signals, such as increased oxidative stress or high lactic acid production, is well documented (53,54). Our data, showing that p53 is upregulated in response to scox KD, but not in response to KD of another Complex IV assembly factor, Surf1, suggest a specific genetic interaction between dp53 and scox. This is corroborated by the dramatic effects observed in the heart structure and function when dp53 is overexpressed in scox KD hearts. Furthermore, the functional and structural defects seen in scox KD hearts could be rescued in dp53-DN OE or dp53 null backgrounds, indicating that the scox-induced defects are mediated by increased p53 expression. Interestingly, opposed to scox KD, the heart structure defects induced by dp53 OE were fully rescued by heart-specific Surf1 KD, further confirming the specificity of the genetic interaction between dp53 and scox.

It has recently been shown that *SCO2* OE induces p53-mediated apoptosis in tumour xenografts and cancer cells (55). Furthermore, *SCO2* KD sensitizes glioma cells to hypoxia-induced apoptosis in a p53-dependent manner and induces necrosis in tumours expressing WT p53 (56), further linking the *SCO2/p53* axis to cell death. In *Drosophila*, there is a *dp53*-mediated upregulation of *Reaper*, *Hid* and *Grim* in response to *scox* KD. This, coupled with the observation that *Reaper* overexpression in the adult heart enhances the structural defects caused by cardiac-specific *scox* KD, suggests that scox normally prevents the triggering of dp53-mediated cell death in cardiomyocytes in stress response. Indeed, we found that there is massive cell death in the skeletal muscle and liver of *Sco2*^{KIKO} mice, supporting the hypothesis that Sco proteins might play this role also in mammals.

We provide evidence that *scox* KD hearts exhibit partial loss of COX activity, with cardiomyocytes undergoing apoptosis. There is evidence from vertebrate and invertebrate models that partial inhibition of mitochondrial respiration promotes longevity and metabolic health due to hormesis (57,58). In fact, it was recently shown that mild interference of the OXPHOS system in *Drosophila* IFMs preserves mitochondrial function, improves muscle performance and increases lifespan through the activation of the mitochondrial unfolded pathway response and IGF/like signalling pathways (59).We speculate that cell death, rather than mitochondrial dysfunction itself, is likely to be the main reason for the profound heart degeneration observed in *TinCΔ4-Gal4>scoxi* flies. Expression of dominant negative *dp53* in *scox* KD hearts rescues dysfunction and cardiac degeneration, and, most importantly, *scox KD in dp53*$^{-/-}$ animals caused no apparent heart defects, leading us to attribute the rescue observed to blockade of the p53 pathway. Indeed, inhibiting apoptosis by *p35* or *Diap1* OE almost completely rescued the morphological *scox* KD phenotype. As *scox* KD in the absence of dp53 causes no symptoms of heart disease, coupled with the inability of *p35* and *Diap1* to completely rescue the morphological phenotype, suggests that, in addition to inducing apoptosis, *dp53* plays a key role in the development of cardiomyopathy.

The fact that heart-specific *Surf1* KD neither upregulates *p53* nor induces apoptosis supports the idea that the partial loss of *scox* function itself triggers *dp53* upregulation and apoptosis, rather than it being a side effect of COX dysfunction and the loss of cellular homeostasis. In this context, it is noteworthy that SCO2 interference in mammalian cells induces p53 re-localization from mitochondria to the nucleus (60). It is therefore tempting to hypothesize that scox might play another role independent of its function as a COX assembly factor, perhaps in redox regulation as suggested previously (7) and that it may act in conjunction with dp53 to fulfil this role. Another issue deserves further attention, the possibility of this interaction being a tissue-specific response. It may be possible that the threshold of COX deficiency tolerated by the heart might be lower than in other tissues, thus the *scox/dp53* genetic interaction may be a tissue-dependent phenomenon or the consequence of a tissue-specific role of *scox*. In fact, it was recently shown that mitochondrial dysfunction in mice is sensed independently from respiratory chain deficiency, leading to tissue-specific activation of cellular stress responses (61). Thus, more work is necessary to test these hypotheses and try to understand how the partial lack of scox induces cell death through dp53.

Although the role of mitochondria in *Drosophila* apoptosis remains unclear, there is strong evidence that, as in mammals, mitochondria play an important role in cell death in flies. The localization of Rpr, Hid and Grim in the mitochondria is essential to promote cell death, and fly mitochondria undergo Rpr-, Hid- and

Drp1-dependent morphological changes and disruption following apoptotic stimulus. Moreover, the participation of the mitochondrial fission protein Drp1 in cell death is conserved in worms and mammals (62). It was recently proposed that p53 plays a role in the opening of the mPTP that induces necrotic cell death (63). According to this model, p53 translocates to the mitochondrial matrix upon ROS stimulation, where it binds cyclophilin D (CypD) to induce mPTP opening independent of proapoptotic Bcl-2 family members Bax and Bak, and in contrast to traditional concepts, independent of Ca^{2+} (reviewed in Ref. 64).

Apoptotic and necrotic pathways have a number of common steps and regulatory factors, including mPTP opening that is thought to provoke mitochondrial swelling and posterior delivery of necrotic factors (65), although *Drosophila* mPTP activation is not accompanied by mitochondrial swelling (66). Interestingly, although the p53 protein triggers mitochondrial outer membrane permeabilization (MOMP) in response to cellular stress in mammals, releasing mitochondrial death factors (67), MOMP in *Drosophila* is more likely a consequence rather than cause of caspase activation (68) and the release of mitochondrial factors does not appear to play a role in apoptosis (69). Thus, in cardiac-specific *scox* KD flies, dp53 might induce mPTP opening to trigger cell death, which in the absence of mitochondrial swelling would result in apoptosis instead of necrosis, as occurs in mammals. *Drosophila* mPTP has been shown to be cyclosporine A (CsA)-insensitive *in vitro* (66), although it was recently shown that CsA administration ameliorates the mitochondrial dysfunction with a severely attenuated ATP and enhanced ROS production displayed by collagen XV/XVIII mutants (70). Interestingly, mice lacking collagen VI display altered mitochondrial structure and spontaneous apoptosis, defects that are caused by mPTP opening and that are normalized *in vivo* by CsA treatment (71).

In summary, we have generated the first animal model to study human Sco-mediated cardiomyopathy in *D. melanogaster*. We demonstrate that cardiac-specific knockdown of *scox* leads to cardiomyocyte cell death in a p53-dependent manner in response to the loss of cell homeostasis and that *dp53* genetically interacts with *scox* and fulfils a key role in the development of cardiomyopathy. Significantly, we show that loss of p53 or inhibition of apoptosis blocks the SCO-induced cardiomyopathy. Moreover, partial loss of SCO2 function also induces apoptosis in liver and skeletal muscle in a $SCO2^{KI/KO}$ mouse model. Therefore, our finding of p53-dependent pathologies due to SCO deficiency appears to be critical for several organ systems in addition to the heart. This information greatly advances our understanding of the mechanisms and consequences involved in SCO deficiency and will likely have a significant impact on our understanding of human metabolic diseases, such as OXPHOS diseases.

Materials and Methods

Fly stocks

UAS-RNAi transgenic fly lines for scox (CG8885; 7861) and Surf1 (CG9943; 100711), referred in the main text and figures as UAS-scoxi and UAS-Surf1i, were obtained from the Vienna *Drosophila* RNAi Centre (VDRC, 72). The cardiac-tissue-specific *TinCΔ4::Gal4* was a kind gift from M. Frasch. The UAS-$p53^{DN}$, UAS-p53 and $p53^{[5A\text{-}1\text{-}4]}$ were obtained from Bloomington, and the UAS-p35, UAS-Diap1 and UAS-rpr lines were kind gifts from M. Calleja.

Drosophila cardiac function and morphology

To assess cardiac function, heartbeat recording of semi-intact hearts was performed as described previously. Videos were analysed using a Semi-automatic Optical Heartbeat Analysis software (sohasoftware.com) to quantify the heart periods, systolic and DI, systolic and diastolic diameters as well as FS reflected in the M-mode recordings (28).

Immunohistochemical staining and respiratory complex activity

Briefly, semi-intact hearts were prepared as described above and phalloidin or SDH and COX activity stained.

ROS and TUNEL staining

Oxidative stress was detected over 1 h with DHE (3 mM final concentration in PBS) and the TUNEL reaction was performed following the manufacturer's instructions (In Situ Cell Death Detection Kit, TMR Red, Roche, Germany).

Real-time PCR

RNA was extracted from 8 to 10 hearts from female flies of each genotype, and it was reverse-transcribed (RT) prior to performing quantitative RT-PCR with the Fast SYBR Green Cells-to-CT™ KIT (Ambion, Applied Biosystems).

Supplementary Material

Supplementary Material is available at *HMG* online.

Acknowledgements

We thank M. Calleja, E. Sanchez Herrero, Developmental Studies Hybridoma Bank and the Vienna *Drosophila* RNAi Center for reagents and fly stocks. We also thank M. Calleja and L. Kaguni for their useful comments on the manuscript and M. Sefton for help preparing the manuscript and English corrections. Heart performance experiments were carried out by L.M. and S.P. at Sanford-Burnham Medical Research Institute under the supervision of K.O. and R.B.

Conflict of Interest statement. None declared.

Funding

This work was supported by grants Direccion General de Investigacion Ciencia y Tecnologia (BFU2007-61711BMC and BFU2010-19551 to M.C.), American Heart Association (Grant in Aid #14GRNT20490239 to K.O.), NASA (NRA NNH12ZTT001N to K.O. and NRA NNH12ZTT001N to R.B.), National Institute of Health (R01 HL054732, P01 AG033461, P01 HL098053 to R.B.), Centre for Biomedical Research on Rare Diseases, Instituto de Salud Carlos III (PI10/0703 and PI13/00556 to R.G.), Comunidad de Madrid (S2010/BMD-2402 to R.G.), Muscular Dystrophy Association to E.A.S., the U.S. Department of Defence (W911F-12-1-0159 to E.A.S.) and J. Willard and Alice S. Marriott Foundation to E.A.S.

References

1. Schaefer, A.M., Taylor, R.W., Turnbull, D.M. and Chinnery, P.F. (2004) The epidemiology of mitochondrial disorders—past, present and future. *Biochim. Biophys. Acta*, **1659**, 115–120.
2. Schiff, M., Ogier de Baulny, H. and Lombes, A. (2011) Neonatal cardiomyopathies and metabolic crises due to oxidative phosphorylation defects. *Semin. Fetal Neonatal Med.*, **16**, 216–221.

3. Soto, I.C., Fontanesi, F., Liu, J. and Barrientos, A. (2012) Biogenesis and assembly of eukaryotic cytochrome c oxidase catalytic core. *Biochim. Biophys. Acta*, **1817**, 883–897.
4. DiMauro, S., Tanji, K. and Schon, E.A. (2012) The many clinical faces of cytochrome c oxidase deficiency. *Adv. Exp. Med. Biol.*, **748**, 341–357.
5. Horng, Y.C., Leary, S.C., Cobine, P.A., Young, F.B., George, G.N., Shoubridge, E.A. and Winge, D.R. (2005) Human Sco1 and Sco2 function as copper-binding proteins. *J. Biol. Chem.*, **280**, 34113–34122.
6. Leary, S.C., Cobine, P.A., Kaufman, B.A., Guercin, G.H., Mattman, A., Palaty, J., Lockitch, G., Winge, D.R., Rustin, P., Horvath, R. *et al.* (2007) The human cytochrome c oxidase assembly factors SCO1 and SCO2 have regulatory roles in the maintenance of cellular copper homeostasis. *Cell Metab.*, **5**, 9–20.
7. Williams, J.C., Sue, C., Banting, G.S., Yang, H., Glerum, D.M., Hendrickson, W.A. and Schon, E.A. (2005) Crystal structure of human SCO1: implications for redox signaling by a mitochondrial cytochrome c oxidase "assembly" protein. *J. Biol. Chem.*, **280**, 15202–15211.
8. Leary, S.C., Antonicka, H., Sasarman, F., Weraarpachai, W., Cobine, P.A., Pan, M., Brown, G.K., Brown, R., Majewski, J., Ha, K.C. *et al.* (2013) Novel mutations in SCO1 as a cause of fatal infantile encephalopathy and lactic acidosis. *Hum. Mutat.*, **34**, 1366–1370.
9. Stiburek, L., Vesela, K., Hansikova, H., Hulkova, H. and Zeman, J. (2009) Loss of function of Sco1 and its interaction with cytochrome c oxidase. *Am. J. Physiol. Cell Physiol.*, **296**, C1218–C1226.
10. Gurgel-Giannetti, J., Oliveira, G., Brasileiro Filho, G., Martins, P., Vainzof, M. and Hirano, M. (2013) Mitochondrial cardioencephalomyopathy due to a novel SCO2 mutation in a Brazilian patient: case report and literature review. *JAMA Neurol.*, **70**, 258–261.
11. Brosel, S., Yang, H., Tanji, K., Bonilla, E. and Schon, E.A. (2010) Unexpected vascular enrichment of SCO1 over SCO2 in mammalian tissues: implications for human mitochondrial disease. *Am. J. Pathol.*, **177**, 2541–2548.
12. Matoba, S., Kang, J.G., Patino, W.D., Wragg, A., Boehm, M., Gavrilova, O., Hurley, P.J., Bunz, F. and Hwang, P.M. (2006) p53 regulates mitochondrial respiration. *Science*, **312**, 1650–1653.
13. Kulawiec, M., Ayyasamy, V. and Singh, K.K. (2009) p53 regulates mtDNA copy number and mitocheckpoint pathway. *J. Carcinog.*, **8**, 8.
14. Park, J.Y., Wang, P.Y., Matsumoto, T., Sung, H.J., Ma, W., Choi, J.W., Anderson, S.A., Leary, S.C., Balaban, R.S., Kang, J.G. *et al.* (2009) p53 improves aerobic exercise capacity and augments skeletal muscle mitochondrial DNA content. *Circ. Res.*, **105**, 705–712. 711 p following 712.
15. Achanta, G., Sasaki, R., Feng, L., Carew, J.S., Lu, W., Pelicano, H., Keating, M.J. and Huang, P. (2005) Novel role of p53 in maintaining mitochondrial genetic stability through interaction with DNA Pol gamma. *EMBO J.*, **24**, 3482–3492.
16. Stambolsky, P., Weisz, L., Shats, I., Klein, Y., Goldfinger, N., Oren, M. and Rotter, V. (2006) Regulation of AIF expression by p53. *Cell Death Differ.*, **13**, 2140–2149.
17. Zhang, C., Lin, M., Wu, R., Wang, X., Yang, B., Levine, A.J., Hu, W. and Feng, Z. (2011) Parkin, a p53 target gene, mediates the role of p53 in glucose metabolism and the Warburg effect. *Proc. Natl Acad. Sci. USA*, **108**, 16259–16264.
18. de la Cova, C., Senoo-Matsuda, N., Ziosi, M., Wu, D.C., Bellosta, P., Quinzii, C.M. and Johnston, L.A. (2014) Supercompetitor status of *Drosophila* Myc cells requires p53 as a fitness sensor to reprogram metabolism and promote viability. *Cell Metab.*, **19**, 470–483.
19. Ocorr, K., Perrin, L., Lim, H.Y., Qian, L., Wu, X. and Bodmer, R. (2007) Genetic control of heart function and aging in *Drosophila*. *Trends Cardiovasc. Med.*, **17**, 177–182.
20. den Hoed, M., Eijgelsheim, M., Esko, T., Brundel, B.J., Peal, D.S., Evans, D.M., Nolte, I.M., Segre, A.V., Holm, H., Handsaker, R.E. *et al.* (2013) Identification of heart rate-associated loci and their effects on cardiac conduction and rhythm disorders. *Nat. Genet.*, **45**, 621–631.
21. Wolf, M.J. and Rockman, H.A. (2011) Drosophila, genetic screens, and cardiac function. *Circ. Res.*, **109**, 794–806.
22. Neely, G.G., Kuba, K., Cammarato, A., Isobe, K., Amann, S., Zhang, L., Murata, M., Elmen, L., Gupta, V., Arora, S. *et al.* (2010) A global *in vivo Drosophila* RNAi screen identifies NOT3 as a conserved regulator of heart function. *Cell*, **141**, 142–153.
23. Porcelli, D., Oliva, M., Duchi, S., Latorre, D., Cavaliere, V., Barsanti, P., Villani, G., Gargiulo, G. and Caggese, C. (2010) Genetic, functional and evolutionary characterization of scox, the *Drosophila melanogaster* ortholog of the human SCO1 gene. *Mitochondrion*, **10**, 433–448.
24. Nguyen, T.B., Ida, H., Shimamura, M., Kitazawa, D., Akao, S., Yoshida, H., Inoue, Y.H. and Yamaguchi, M. (2014) Role of SCOX in determination of *Drosophila melanogaster* lifespan. *Am. J. Cancer Res.*, **4**, 325–336.
25. Peralta, S., Clemente, P., Sanchez-Martinez, A., Calleja, M., Hernandez-Sierra, R., Matsushima, Y., Adan, C., Ugalde, C., Fernandez-Moreno, M.A., Kaguni, L.S. *et al.* (2012) Coiled coil domain-containing protein 56 (CCDC56) is a novel mitochondrial protein essential for cytochrome c oxidase function. *J. Biol. Chem.*, **287**, 24174–24185.
26. Tiefenbock, S.K., Baltzer, C., Egli, N.A. and Frei, C. (2010) The *Drosophila* PGC-1 homologue Spargel coordinates mitochondrial activity to insulin signalling. *EMBO J.*, **29**, 171–183.
27. Masoud, W.G., Ussher, J.R., Wang, W., Jaswal, J.S., Wagg, C.S., Dyck, J.R., Lygate, C.A., Neubauer, S., Clanachan, A.S. and Lopaschuk, G.D. (2014) Failing mouse hearts utilize energy inefficiently and benefit from improved coupling of glycolysis and glucose oxidation. *Cardiovasc. Res.*, **101**, 30–38.
28. Fink, M., Callol-Massot, C., Chu, A., Ruiz-Lozano, P., Izpisua Belmonte, J.C., Giles, W., Bodmer, R. and Ocorr, K. (2009) A new method for detection and quantification of heartbeat parameters in *Drosophila*, zebrafish, and embryonic mouse hearts. *Biotechniques*, **46**, 101–113.
29. Tay, S.K., Shanske, S., Kaplan, P. and DiMauro, S. (2004) Association of mutations in SCO2, a cytochrome c oxidase assembly gene, with early fetal lethality. *Arch. Neurol.*, **61**, 950–952.
30. St-Pierre, J., Buckingham, J.A., Roebuck, S.J. and Brand, M.D. (2002) Topology of superoxide production from different sites in the mitochondrial electron transport chain. *J. Biol. Chem.*, **277**, 44784–44790.
31. Yang, H., Brosel, S., Acin-Perez, R., Slavkovich, V., Nishino, I., Khan, R., Goldberg, I.J., Graziano, J., Manfredi, G. and Schon, E.A. (2010) Analysis of mouse models of cytochrome c oxidase deficiency owing to mutations in Sco2. *Hum. Mol. Genet.*, **19**, 170–180.
32. Sung, H.J., Ma, W., Wang, P.Y., Hynes, J., O'Riordan, T.C., Combs, C.A., McCoy, J.P. Jr., Bunz, F., Kang, J.G. and Hwang, P.M. (2010) Mitochondrial respiration protects against oxygen-associated DNA damage. *Nat. Commun.*, **1**, 5.

33. Berkers, C.R., Maddocks, O.D., Cheung, E.C., Mor, I. and Vousden, K.H. (2013) Metabolic regulation by p53 family members. *Cell Metab.*, **18**, 617–633.
34. Birks, E.J., Latif, N., Enesa, K., Folkvang, T., Luong Le, A., Sarathchandra, P., Khan, M., Ovaa, H., Terracciano, C.M., Barton, P.J. *et al.* (2008) Elevated p53 expression is associated with dysregulation of the ubiquitin-proteasome system in dilated cardiomyopathy. *Cardiovasc. Res.*, **79**, 472–480.
35. Nakamura, H., Matoba, S., Iwai-Kanai, E., Kimata, M., Hoshino, A., Nakaoka, M., Katamura, M., Okawa, Y., Ariyoshi, M., Mita, Y. *et al.* (2012) p53 promotes cardiac dysfunction in diabetic mellitus caused by excessive mitochondrial respiration-mediated reactive oxygen species generation and lipid accumulation. *Circ. Heart Fail.*, **5**, 106–115.
36. Ollmann, M., Young, L.M., Di Como, C.J., Karim, F., Belvin, M., Robertson, S., Whittaker, K., Demsky, M., Fisher, W.W., Buchman, A. *et al.* (2000) Drosophila p53 is a structural and functional homolog of the tumor suppressor p53. *Cell*, **101**, 91–101.
37. Zordan, M.A., Cisotto, P., Benna, C., Agostino, A., Rizzo, G., Piccin, A., Pegoraro, M., Sandrelli, F., Perini, G., Tognon, G. *et al.* (2006) Post-transcriptional silencing and functional characterization of the *Drosophila melanogaster* homolog of human Surf1. *Genetics*, **172**, 229–241.
38. Brodsky, M.H., Weinert, B.T., Tsang, G., Rong, Y.S., McGinnis, N.M., Golic, K.G., Rio, D.C. and Rubin, G.M. (2004) *Drosophila melanogaster* MNK/Chk2 and p53 regulate multiple DNA repair and apoptotic pathways following DNA damage. *Mol. Cell. Biol.*, **24**, 1219–1231.
39. Fan, Y., Lee, T.V., Xu, D., Chen, Z., Lamblin, A.F., Steller, H. and Bergmann, A. (2010) Dual roles of *Drosophila* p53 in cell death and cell differentiation. *Cell Death Differ.*, **17**, 912–921.
40. Hay, B.A., Wolff, T. and Rubin, G.M. (1994) Expression of baculovirus P35 prevents cell death in *Drosophila*. *Development*, **120**, 2121–2129.
41. Wang, S.L., Hawkins, C.J., Yoo, S.J., Muller, H.A. and Hay, B.A. (1999) The *Drosophila* caspase inhibitor DIAP1 is essential for cell survival and is negatively regulated by HID. *Cell*, **98**, 453–463.
42. Schwarz, K., Siddiqi, N., Singh, S., Neil, C.J., Dawson, D.K. and Frenneaux, M.P. (2014) The breathing heart—mitochondrial respiratory chain dysfunction in cardiac disease. *Int. J. Cardiol.*, **171**, 134–143.
43. Shires, S.E. and Gustafsson, A.B. (2015) Mitophagy and heart failure. *J. Mol. Med. (Berl.)*, **93**, 253–262.
44. Papadopoulou, L.C., Sue, C.M., Davidson, M.M., Tanji, K., Nishino, I., Sadlock, J.E., Krishna, S., Walker, W., Selby, J., Glerum, D.M. *et al.* (1999) Fatal infantile cardioencephalomyopathy with COX deficiency and mutations in SCO2, a COX assembly gene. *Nat. Genet.*, **23**, 333–337.
45. Nascimben, L., Ingwall, J.S., Lorell, B.H., Pinz, I., Schultz, V., Tornheim, K. and Tian, R. (2004) Mechanisms for increased glycolysis in the hypertrophied rat heart. *Hypertension*, **44**, 662–667.
46. Honzik, T., Tesarova, M., Magner, M., Mayr, J., Jesina, P., Vesela, K., Wenchich, L., Szentivanyi, K., Hansikova, H., Sperl, W. *et al.* (2012) Neonatal onset of mitochondrial disorders in 129 patients: clinical and laboratory characteristics and a new approach to diagnosis. *J. Inherit. Metab. Dis.*, **35**, 749–759.
47. Dorn, G.W. II, Clark, C.F., Eschenbacher, W.H., Kang, M.Y., Engelhard, J.T., Warner, S.J., Matkovich, S.J. and Jowdy, C.C. (2011) MARF and Opa1 control mitochondrial and cardiac function in *Drosophila*. *Circ. Res.*, **108**, 12–17.
48. Shahrestani, P., Leung, H.T., Le, P.K., Pak, W.L., Tse, S., Ocorr, K. and Huang, T. (2009) Heterozygous mutation of *Drosophila* Opa1 causes the development of multiple organ abnormalities in an age-dependent and organ-specific manner. *PLoS ONE*, **4**, e6867.
49. Lin, M.T. and Beal, M.F. (2006) Mitochondrial dysfunction and oxidative stress in neurodegenerative diseases. *Nature*, **443**, 787–795.
50. Leadsham, J.E., Sanders, G., Giannaki, S., Bastow, E.L., Hutton, R., Naeimi, W.R., Breitenbach, M. and Gourlay, C.W. (2013) Loss of cytochrome c oxidase promotes RAS-dependent ROS production from the ER resident NADPH oxidase, Yno1p, in yeast. *Cell Metab.*, **18**, 279–286.
51. Fukui, H., Diaz, F., Garcia, S. and Moraes, C.T. (2007) Cytochrome c oxidase deficiency in neurons decreases both oxidative stress and amyloid formation in a mouse model of Alzheimer's disease. *Proc. Natl Acad. Sci. USA*, **104**, 14163–14168.
52. Vousden, K.H. and Prives, C. (2009) Blinded by the light: the growing complexity of p53. *Cell*, **137**, 413–431.
53. Olovnikov, I.A., Kravchenko, J.E. and Chumakov, P.M. (2009) Homeostatic functions of the p53 tumor suppressor: regulation of energy metabolism and antioxidant defense. *Semin. Cancer Biol.*, **19**, 32–41.
54. Zhuang, J., Ma, W., Lago, C.U. and Hwang, P.M. (2012) Metabolic regulation of oxygen and redox homeostasis by p53: lessons from evolutionary biology? *Free Radic. Biol. Med.*, **53**, 1279–1285.
55. Madan, E., Gogna, R., Kuppusamy, P., Bhatt, M., Mahdi, A.A. and Pati, U. (2013) SCO2 induces p53-mediated apoptosis by Thr845 phosphorylation of ASK-1 and dissociation of the ASK-1-Trx complex. *Mol. Cell Biol.*, **33**, 1285–1302.
56. Wanka, C., Steinbach, J.P. and Rieger, J. (2012) Tp53-induced glycolysis and apoptosis regulator (TIGAR) protects glioma cells from starvation-induced cell death by up-regulating respiration and improving cellular redox homeostasis. *J. Biol. Chem.*, **287**, 33436–33446.
57. Liu, X., Jiang, N., Hughes, B., Bigras, E., Shoubridge, E. and Hekimi, S. (2005) Evolutionary conservation of the clk-1-dependent mechanism of longevity: loss of mclk1 increases cellular fitness and lifespan in mice. *Genes Dev.*, **19**, 2424–2434.
58. Rea, S.L., Ventura, N. and Johnson, T.E. (2007) Relationship between mitochondrial electron transport chain dysfunction, development, and life extension in *Caenorhabditis elegans*. *PLoS Biol.*, **5**, e259.
59. Owusu-Ansah, E., Song, W. and Perrimon, N. (2013) Muscle mitohormesis promotes longevity via systemic repression of insulin signaling. *Cell*, **155**, 699–712.
60. Zhuang, J., Wang, P.Y., Huang, X., Chen, X., Kang, J.G. and Hwang, P.M. (2013) Mitochondrial disulfide relay mediates translocation of p53 and partitions its subcellular activity. *Proc. Natl Acad. Sci. USA*, **110**, 17356–17361.
61. Dogan, S.A., Pujol, C., Maiti, P., Kukat, A., Wang, S., Hermans, S., Senft, K., Wibom, R., Rugarli, E.I. and Trifunovic, A. (2014) Tissue-specific loss of DARS2 activates stress responses independently of respiratory chain deficiency in the heart. *Cell Metab.*, **19**, 458–469.
62. Abdelwahid, E., Rolland, S., Teng, X., Conradt, B., Hardwick, J.M. and White, K. (2011) Mitochondrial involvement in cell death of non-mammalian eukaryotes. *Biochim. Biophys. Acta*, **1813**, 597–607.
63. Vaseva, A.V., Marchenko, N.D., Ji, K., Tsirka, S.E., Holzmann, S. and Moll, U.M. (2012) p53 opens the mitochondrial

permeability transition pore to trigger necrosis. *Cell*, **149**, 1536–1548.
64. Siemen, D. and Ziemer, M. (2013) What is the nature of the mitochondrial permeability transition pore and what is it not? *IUBMB Life*, **65**, 255–262.
65. Nikoletopoulou, V., Markaki, M., Palikaras, K. and Tavernarakis, N. (2013) Crosstalk between apoptosis, necrosis and autophagy. *Biochim. Biophys. Acta*, **1833**, 3448–3459.
66. von Stockum, S., Basso, E., Petronilli, V., Sabatelli, P., Forte, M.A. and Bernardi, P. (2011) Properties of Ca(2+) transport in mitochondria of *Drosophila melanogaster*. *J. Biol. Chem.*, **286**, 41163–41170.
67. Danial, N.N. and Korsmeyer, S.J. (2004) Cell death: critical control points. *Cell*, **116**, 205–219.
68. Abdelwahid, E., Yokokura, T., Krieser, R.J., Balasundaram, S., Fowle, W.H. and White, K. (2007) Mitochondrial disruption in *Drosophila* apoptosis. *Dev. Cell*, **12**, 793–806.
69. Means, J.C., Muro, I. and Clem, R.J. (2006) Lack of involvement of mitochondrial factors in caspase activation in a *Drosophila* cell-free system. *Cell Death Differ.*, **13**, 1222–1234.
70. Momota, R., Narasaki, M., Komiyama, T., Naito, I., Ninomiya, Y. and Ohtsuka, A. (2013) *Drosophila* type XV/XVIII collagen mutants manifest integrin mediated mitochondrial dysfunction, which is improved by cyclosporin A and losartan. *Int. J. Biochem. Cell Biol.*, **45**, 1003–1011.
71. Irwin, W.A., Bergamin, N., Sabatelli, P., Reggiani, C., Megighian, A., Merlini, L., Braghetta, P., Columbaro, M., Volpin, D., Bressan, G.M. *et al.* (2003) Mitochondrial dysfunction and apoptosis in myopathic mice with collagen VI deficiency. *Nat. Genet.*, **35**, 367–371.
72. Dietzl, G., Chen, D., Schnorrer, F., Su, K.C., Barinova, Y., Fellner, M., Gasser, B., Kinsey, K., Oppel, S., Scheiblauer, S. *et al.* (2007) A genome-wide transgenic RNAi library for conditional gene inactivation in Drosophila. *Nature*, **448**, 151–156.